Published in final edited form as:
J Clin Exp Oncol. 2013 ; 2(2): . doi:10.4172/2324-9110.1000106.

Proximal-type Epithelioid Sarcoma of the Head and Neck (HN): A Study with Immunohistochemical and Molecular Analysis of SMARCB1

Renee Frank[1], **Navid Sadri**[1], **Tricia Bhatti**[2], **Jaclyn A Biegel**[3], **Virginia A LiVolsi**[1], and **Paul J Zhang**[1,*]

[1]Anatomic Pathology, Department of Pathology and Laboratory Medicine, Hospital of the University of Pennsylvania, Philadelphia, Pennsylvania, USA

[2]Anatomic Pathology, Department of Pathology and Laboratory Medicine, Children's Hospital of Philadelphia, Philadelphia, Pennsylvania, USA

[3]Departments of Pediatrics and Pathology and Laboratory Medicine, Children's Hospital of Philadelphia and Perelman School of Medicine at the University of Pennsylvania, Philadelphia, Pennsylvania, USA

Abstract

Proximal-type epithelioid sarcoma is an aggressive variant of epithelioid sarcoma most often occurring in soft tissues of the proximal limbs, characterized by polygonal cells, marked nuclear atypia, and varied rhabdoid features. Malignant rhabdoid tumor is an aggressive, well characterized entity typically with rhabdoid morphology and involving the kidney of pediatric patients. Rarely, tumors with morphologic and biologic features identical to those in kidney occur in extra-renal sites and are regarded as an extrarenal presentation of the same entity in kidney, named malignant extra-renal rhabdoid tumor. Morphologic and immunophenotypical similarities between proximal-type epithelioid sarcoma and malignant rhabdoid tumor pose a diagnostic challenge and may suggest a relationship between the two. Both tumors are characterized by loss of SMARCB1 (INI1/BAF47/SNF5) expression; however, the molecular events involved differ. Here we describe the immunohistochemical and molecular analysis of three head and neck tumors with morphologic features shared by proximal-type epithelioid sarcoma and malignant rhabdoid tumor. All tumors showed loss of SMARCB1expression. Direct sequencing of the promoter and nine coding exons of *SMARCB1*, multiplex ligation-dependent probe amplification, and whole genome single nucleotide polymorphism array were performed on the two adult cases and showed only a heterozygous deletion of chromosome 22 in a minority of cells in one of the cases. Though rare, proximal-type epithelioid sarcoma could occur in the head and neck and should be differentiated from other epithelioid tumors by the loss of SMARCB1 expression. The lack of detectable genetic alteration in the *SMARCB1* locus in head and neck proximal-type epithelioid sarcoma warrants further investigation into the molecular mechanism underlying loss of SMARCB1 expression.

[*]Corresponding author: Paul J Zhang, Hospital of the University of Pennsylvania, 3400 Spruce Street, 6th Floor Founders Building, Philadelphia, PA 19104, USA, Tel: 215-662-6526, Fax: 215-662-3238, pjz@mail.med.upenn.edu.

The authors have no conflicts of interest to disclose.

Keywords

Proximal epithelioid sarcoma; Malignant extra-renal rhabdoid tumor; *INI1/SMARCB1*; Multiplex ligation-dependent probe amplification (MLPA); Single nucleotide polymorphism (SNP) array

Introduction

Epithelioid sarcoma is a rare aggressive soft tissue sarcoma first described by Laskowski in 1961 and then recognized as a distinct entity by Enzinger in 1970 [1]. The conventional or "distal" type epithelioid sarcoma typically occurs in the distal extremities in young adults as a slow-growing soft tissue neoplasm with an infiltrative growth pattern along fascial planes with a high rate of local recurrence and metastases [2]. Proximal-type epithelioid sarcoma (PES) is a more aggressive variant of epithelioid sarcoma occurring most often in soft tissues of the proximal limbs, including the pelvis and perineal regions, in young to middle aged adults. This variant is histologically characterized by sheets of larger polygonal cells with marked nuclear atypia and varied rhabdoid features [3,4]. These characteristic "rhabdoid cells" have been described in other soft tissue sarcomas, most prominently in malignant rhabdoid tumor (MRT), and their presence is correlated with a worse prognosis [5–7]. Although PES is currently distinguished from MRT as a specific diagnostic entity, the shared rhabdoid features have led some to suggest that these tumors belong along a spectrum of poorly differentiated neoplasms with rhabdoid features [3,8].

Morphologic and immunohistochemical (IHC) similarities between PES and malignant extra-renal rhabdoid tumors (MRT) pose a diagnostic challenge. Both tumors are extremely rare within the head and neck and both are characterized by loss of SMARCB1 expression. *SMARCB1*, located on chromosome 22q11.2, was first identified as an interactor protein of HIV integrase [9]. It is an invariant subunit of the SWI/SNF-related chromatin remodeling complex that regulates transcription and acts as an indirect suppressor of the cell cycle [10,11]. More recently, *SMARCB1* has been defined as a tumor suppressor gene. The molecular events mediating this loss of expression might differ between these two entities, with point mutations more common in MRT and deletions in PES [12,13]. We report histologic and immunohistochemical analysis of three cases of PES within the head and neck, with two undergoing molecular analyses for alterations at the DNA level that may mediate the loss of SMARCB1 expression.

Materials and Methods

Histologic and immunohistochemical sections

Biopsies and resection specimens were fixed in 10% formalin, embedded in paraffin and sectioned at 5 μm for hematoxylin and eosin (H&E) staining and immunohistochemical analysis. Commercially available antibodies, as shown in Table 1, for AE1/3 PanCK, CAM5.2 CDX2, CK20, p63, CK5/6, CEA, myogenin, desmin, EMA, SMA, CD31, CD34, D2-40, NSE, GFAP, CD163, CD68, CD1a, LCA, E-cadherin, B72.3 (BRST2), GCD-FP-15 (BRST3), TDT, chromogranin, synaptophysin, calretinin, inhibin, TLE-1, BAF47 (SMARCB1), PLAP, WT-1, OCT4, TTF-1, EBER, S100, HMB-45, and melan-A were used in the analysis of the three tumors at the time of the diagnosis. FISH analysis for *MDM2* amplification and *SYT* translocation were performed with commercially available probes (Abbott Laboratories, USA) according to the manufacturer's instructions.

Molecular analysis

Molecular analysis was performed at the time of the diagnosis as an ancillary test to confirm the diagnosis. Fresh frozen tissue samples were collected from the two adult resection

specimens. Genomic DNA was extracted using a commercially available kit (Gentra Puregene DNA isolation kit, Quigen, Inc., Valencia, CA) and used for mutation detection, multiplex ligation-dependent probe amplification (MLPA), and single nucleotide polymorphism (SNP) array analysis according to previously published protocols [14–16].

Case Presentations

Case 1

A 43 year-old man with a history of ulcerative colitis, chronic kidney disease, and right eye blindness secondary to polyarteritis nodosa, presented with one week of left eye pain and protrusion. A head computed tomography (CT) demonstrated a 2.4 x 3.4 x 1.5 cm left retro-orbital mass extending from the superior rectus muscle to the orbital apex. A lateral orbitotomy was performed at that time. The patient refused an orbital exenteration and chemotherapy and was lost to follow-up. The patient returned with a new right middle lobe lung lesion on CT, and subsequently received five cycles of Ifosfamide and Adriamycin chemotherapy. Two years after the first presentation the patient underwent a second lateral orbitotomy and superior rectus muscle resection to remove approximately 90–95% of the mass.

Histologically, the tumors from the first orbitotomy specimen consisted of poorly differentiated, discohesive, medium-sized polygonal and short spindled cells with nuclear irregularity and atypia. Some of the tumor cells featured eccentric nuclei and abundant eosinophilic cytoplasm (Figure 1). The recurrent post treatment tumor in the second lateral orbitotomy specimen consisted of poorly differentiated, discohesive, medium-sized polygonal and short spindled cells, loosely arranged in myxoid stroma or individually admixed with exuberant foamyv histiocytes as seen in Figure 1C. Mitotic figures were rare in both specimens and no tumor necrosis was seen. The tumor excised by the first orbitotomy specimen showed a complete loss of SMARCB1 nuclear expression but focal loss of SMARCB1 expression in the second orbitotomy specimen. Tumors of both specimens showed strong desmin positivity and D2-40 expression. The first resected tumor showed no cytokeratin expression while the second resection specimen exhibited strong cytokeratin staining. The remainder of an extensive IHC panel (see methods) was negative, including S100 and p63, arguing against a myoepithelial carcinoma. A FISH assay for *MDM2* amplification as seen in dedifferentiated liposarcoma was negative.

No duplications or deletions were detected in the coding sequence of the *SMARCB1* gene by the MLPA assay. Direct sequencing of the coding and promoter region of the *SMARCB1* gene revealed no mutations. Whole gene SNP array studies revealed no genetic alterations.

Case 2

An otherwise healthy 71 year-old female reported to her family physician with severe left sided headaches, facial swelling, and intermittent epistaxis. A nasolaryngoscopy was performed and showed a mass within the left nasal cavity. An MRI revealed a 3.5 x 3.0 x 2.9 cm mass within the left nasal cavity with complete opacification of the left maxillary, sphenoid and ethmoid sinus secondary to the mass. Additionally the patient had multiple enlarged cervical lymph nodes concerning for metastasis. She subsequently underwent an intranasal rhinotomy, ethmoidectomy, spenoidectomy, and resection of the skull base tumor.

Histologically, the tumor consisted of sheets of round medium to large-sized, monotonous polygonal cells with abundant eosinophilic cytoplasm and eccentric nuclei with small prominent nucleoli (Figure 2). Mitoses were rare and little necrosis was noted. IHC staining showed that the neoplastic cells were positive for PANCK, EMA, E-cadherin and B72.3.

The neoplastic cells showed consistent loss of SMARCB1 expression (Figure 3). Myogenin, desmin, GCD-FP-15, chromogranin, and synaptophysin were all negative.

The MLPA assay and direct sequencing revealed no genetic alterations in the promoter region and coding sequence of the *SMARCB1* gene locus. Whole genome SNP array studies revealed a small population of cells with gain of chromosome 7 and a heterozygous deletion of chromosome 22.

Case 3

A previously healthy 9-year old female presented with a rapidly enlarging posterior paramedian neck mass. On examination the protuberant mass extended from the right side of the neck to the angle of her right mandible and was slightly tender to palpation. A CT scan of the primary site revealed a right paramedian and paravertebral heterogeneous neck mass with punctate calcifications measuring 8 x 6 x 5 cm without bony involvement or spinal extension. Further imaging demonstrated multiple bilateral pulmonary nodules which were not PET-avid. A bilateral renal ultrasound was normal. A biopsy of the neck mass was performed prior to initiating chemotherapy.

Histologically, the high grade neoplasm was composed of undifferentiated cells with varying amounts of eosinophilic cytoplasm, vesicular chromatin, and prominent nucleoli. Many apoptotic bodies and foci or intratumoral necrosis were seen. A minority population of cells exhibited a rhabdoid appearance with eccentric nuclei with abundant cytoplasm (Figure 4). The tumor cells were positive for EMA, TLE-1, SMA, and AE1/3. AE1/3 and SMA showed focal membranous and cytoplasmic staining, respectively. There was loss of nuclear SMARCB1 expression. The tumor cells were negative for MIC2, myogenin, desmin, TDT, CD34, WT-1 and tyrosine hydroxylase. FISH analysis for a *SYT* translocation, as seen in synovial sarcoma, was negative.

Case follow-up

The patient described in case 1, after a 36 month followup, has developed filamentary keratitis of the left eye and has developed stable hypermetabolic activity in the midline superficial nasopharyngeal soft tissue visualized on interval PET/CT scans. On follow-up examinations over 29 months, the female patient in case 2 is well clinically and radiologically with no evidence of disease. Unfortunately, follow-up information on the pediatric patient in case 3 is currently unknown.

Discussion

In this cohort, we have described a soft tissue entity with aggressive clinical features occurring in the head and neck region. Histologically, although the cases reported here shows variable morphologic features, the common histologic features of these tumors are sheets of polygonal cells with variable intervening stroma and variable degree of rhabdoid morphology. Other variants of cell type such as round cell, epithelioid and undifferentiated cytology can be seen in tumor with less classic rhabdoid morphology. The differential of these tumors can include poorly differentiated or undifferentiated round cell tumor such as sinonasal undifferentiated carcinomas, rhabdomyosarcoma, large cell lymphoma, EWS/PNET, MRT, proximal epithelioid sarcoma and other sarcomas with epithelioid/rhabdoid features. The immunohistochemical profile showed diffuse positivity for cytokeratin markers. Myogenin and CD31 were both negative, excluding rhabdomyosarcoma and epithelioid angiosarcoma, respectively. IHC staining revealed compete loss of expression of SMARCB1, which is normally ubiquitously expressed, as seen in normal stromal cells

(Figures 3 and 4). The morphologic features and loss of SMARCB1 expression are consistent with a tumor within the PES family.

Mutation analysis by direct sequencing of the promoter and 9 exons of *SMARCB1*, multiplex ligation-dependent probe amplification (MLPA), and whole genome single nucleotide polymorphism (SNP) array were performed on the two adult cases. No mutations were observed. One of the two tumors showed a heterozygous deletion of chromosome 22 in a minority of cells by whole genome SNP array. Given the low level of tumor cell content, this does not exclude the possibility of a mutation present on the remaining allele. Alternatively, a mutation in a non-coding region of the locus may be present, which would not be detected with assays employed.

Biallelic inactivation of *SMARCB1* has been reported in approximately 98% of rhabdoid tumors of the kidney, brain and soft tissues [14,17]. Reintroduction of the *SMARCB1* gene in MRT cell lines blocks cellular proliferation and induces cellular senescence [18]. Immunohistochemically, these tumors characteristically lose SMARCB1 nuclear reactivity, which has been used as a diagnostic marker to differentiate the group of tumors from their mimics. Up to 93% of proximal type and 76% of conventional type epithelioid sarcomas show loss of SMARCB1 protein expression by IHC. In addition to the vast majority of classic rhabdoid tumors, two larger series have demonstrated that 90% of proximal type and 86% of conventional type epithelioid sarcomas show loss of SMARCB1 protein expression by IHC [2,19].

In a small report, molecular analysis of PES revealed a genomic deletion of the *SMARCB1* locus in five of six cases which correlated with the downregulation of protein and mRNA expression [13]. In another report, spectral karyotyping analysis of six PES revealed the presence of rearrangements on chromosome 22q in five of them, with two cases showing a similar t (10;22) chromosome translocation [10]. However, alterations at the DNA level have been more elusive with only 10.3% (4/39) of the reported cases showing a coding sequence mutation [12]. Evaluation of detectable molecular alterations suggests that the spectrum of *SMARCB1* alterations may be biased to deletions, some of which arise as a consequence of unbalanced translocations [20]. Furthermore, there is a heterogeneous distribution of the deletions observed thus far in epithelioid sarcomas. The oncogenic role of the heterogeneous distribution observed thus far in epithelioid sarcoma is unclear and led to the suggestion that at least in some cases they represent relevant secondary tumor–associated changes and not the primary event causing the tumor [13].

In stark contrast, only 2% of MRT cases assayed lack identified genomic alterations of the *SMARCB1* locus [12,16]. MRTs, similar to PES, have a high frequency of homozygous deletions. Analysis of the methylation status of the *SMARCB1* promoter in MRTs provided no evidence for hypermethylation, making this mechanism unlikely in MRT [21]. Other neoplasms, such as epithelioid malignant peripheral nerve sheath tumor and renal medullary carcinoma have been reported to demonstrate loss of expression of SMARCB1, although the number of cases with inactivating gene deletions or mutations of *SMARCB1* is limited [15,22,23]. The molecular events underlying loss of SMARCB1 expression in PES, MRT and other tumors with epithelioid/rhabdoid features in cases without identifiable genomic deletion or translocation, need to be better characterized, including posttranscriptional mechanisms of inactivation [13]. Furthermore, investigation of SMARCB1 expression in well-characterized head and neck tumors and derived cell lines will be valuable in better understanding oncogenic mechanisms regulating SMARCB1 expression, as well as, in distinguishing PES from other head and neck tumors.

While PES is considered a distinct diagnostic entity in contrast to MRT, some investigators have proposed that PES is an entity along a spectrum of poorly differentiated neoplasms with rhabdoid features and phenotype [3,8]. The distinction of PES from MRT is supported by the observation that the prognosis of patients with MRT is significantly worse than in patients with PES [12]. There is a strong association of deletions with PES, although that is also the case for other extra-renal, non-CNS rhabdoid tumors. It is possible that the molecular genetic alterations are similar among these entities, but that the cell of origin is different, thus accounting for the better prognosis among adult patients.

Due to the strong epithelioid phenotype, limited myoid differentiation, molecular findings and overall clinical presentation, we favor the diagnosis of PES over MRT for these three cases. Meanwhile, due to the similar morphologic features and loss of SMARCB1 expression in these tumors, PES and MRT can certainly be two different presentation of a specific morphologic spectrum spanning at one end with more epithelioid phenotype to the other with more rhabdoid phenotype of a neoplastic process related to the *SMARCB1* alteration regardless of the underlying molecular events leading to its inactivation. Clinical outcome study with an investigation for alternative mutational events in the *SMARCB1* locus in larger series of cases might further clarify whether PES and MRT exist as a shared phenotype of distinct entities or exist on a spectrum of a single disease.

Although proximal epithelial sarcomas and MRT have been reported to demonstrate loss of expression of SMARCB1, inactivating gene deletions or mutations have only been described in a subset of these cases [15]. It will be of interest to further characterize the molecular changes in these cases in search of alternative mutational events, such as epigenetic silencing, intronic mutations, RNA editing, or post-transcriptional control. Though rare, PES could occur in HN and should be differentiated from other tumors with epithelioid/epithelial differentiation by absence of SMARCB1 staining. The lack of known *SMARCB1* mutation and deletion in a HN PES warrants further study to investigate alternative mechanisms of inactivation of this gene.

Acknowledgments

The authors wish to thank Laura Tooke and Katherine Eaton for technical assistance. The study was supported in part by a grant from the NIH (CA46274) to JAB. This data was presented in part at the United States and Canadian Academy of Pathology conference, Vancouver, Canada in March 2012.

References

1. Enzinger FM. Epitheloid sarcoma. A sarcoma simulating a granuloma or a carcinoma. Cancer. 1970; 26:1029–1041. [PubMed: 5476785]
2. Hornick JL, Dal Cin P, Fletcher CD. Loss of INI1 expression is characteristic of both conventional and proximal-type epithelioid sarcoma. Am J Surg Pathol. 2009; 33:542–550. [PubMed: 19033866]
3. Guillou L, Wadden C, Coindre JM, Krausz T, Fletcher CD. “Proximal-type” epithelioid sarcoma, a distinctive aggressive neoplasm showing rhabdoid features. Clinicopathologic, immunohistochemical, and ultrastructural study of a series. Am J Surg Pathol. 1997; 21:130–146. [PubMed: 9042279]
4. Izumi T, Oda Y, Hasegawa T, Nakanishi Y, Iwasaki H, et al. Prognostic significance of dysadherin expression in epithelioid sarcoma and its diagnostic utility in distinguishing epithelioid sarcoma from malignant rhabdoid tumor. Mod Pathol. 2006; 19:820–831. [PubMed: 16557275]
5. Miettinen M, Fanburg-Smith JC, Virolainen M, Shmookler BM, Fetsch JF. Epithelioid sarcoma: an immunohistochemical analysis of 112 classical and variant cases and a discussion of the differential diagnosis. Hum Pathol. 1999; 30:934–942. [PubMed: 10452506]

6. Oshiro Y, Shiratsuchi H, Tamiya S, Oda Y, Toyoshima S, et al. Extraskeletal Myxoid Chondrosarcoma with Rhabdoid Features, with Special Reference to Its Aggressive Behavior. Int J Surg Pathol. 2000; 8:145–152. [PubMed: 11493979]
7. Tsuneyoshi M, Daimaru Y, Hashimoto H, Enjoji M. The existence of rhabdoid cells in specified soft tissue sarcomas. Histopathological, ultrastructural and immunohistochemical evidence. Virchows Arch A Pathol Anat Histopathol. 1987; 411:509–514. [PubMed: 2445098]
8. Hasegawa T, Matsuno Y, Shimoda T, Umeda T, Yokoyama R, et al. Proximal-type epithelioid sarcoma: a clinicopathologic study of 20 cases. Mod Pathol. 2001; 14:655–663. [PubMed: 11454997]
9. Kalpana GV, Marmon S, Wang W, Crabtree GR, Goff SP. Binding and stimulation of HIV-1 integrase by a human homolog of yeast transcription factor SNF5. Science. 1994; 266:2002–2006. [PubMed: 7801128]
10. Imbalzano AN, Jones SN. Snf5 tumor suppressor couples chromatin remodeling, checkpoint control, and chromosomal stability. Cancer Cell. 2005; 7:294–295. [PubMed: 15837618]
11. Kingston RE, Bunker CA, Imbalzano AN. Repression and activation by multiprotein complexes that alter chromatin structure. Genes Dev. 1996; 10:905–920. [PubMed: 8608939]
12. Kohashi K, Izumi T, Oda Y, Yamamoto H, Tamiya S, et al. Infrequent SMARCB1/INI1 gene alteration in epithelioid sarcoma: a useful tool in distinguishing epithelioid sarcoma from malignant rhabdoid tumor. Hum Pathol. 2009; 40:349–355. [PubMed: 18973917]
13. Modena P, Lualdi E, Facchinetti F, Galli L, Teixeira MR, et al. SMARCB1/INI1 tumor suppressor gene is frequently inactivated in epithelioid sarcomas. Cancer Res. 2005; 65:4012–4019. [PubMed: 15899790]
14. Biegel JA, Zhou JY, Rorke LB, Stenstrom C, Wainwright LM, et al. Germ-line and acquired mutations of INI1 in atypical teratoid and rhabdoid tumors. Cancer Res. 1999; 59:74–79. [PubMed: 9892189]
15. Eaton KW, Tooke LS, Wainwright LM, Judkins AR, Biegel JA. Spectrum of SMARCB1/INI1 mutations in familial and sporadic rhabdoid tumors. Pediatr Blood Cancer. 2011; 56:7–15. [PubMed: 21108436]
16. Jackson EM, Sievert AJ, Gai X, Hakonarson H, Judkins AR, et al. Genomic analysis using high-density single nucleotide polymorphism-based oligonucleotide arrays and multiplex ligation-dependent probe amplification provides a comprehensive analysis of INI1/SMARCB1 in malignant rhabdoid tumors. Clin Cancer Res. 2009; 15:1923–1930. [PubMed: 19276269]
17. Versteege I, Sevenet N, Lange J, Rousseau-Merck MF, Ambros P, et al. Truncating mutations of hSNF5/INI1 in aggressive paediatric cancer. Nature. 1998; 394:203–206. [PubMed: 9671307]
18. Betz BL, Strobeck MW, Reisman DN, Knudsen ES, Weissman BE. Re-expression of hSNF5/INI1/BAF47 in pediatric tumor cells leads to G1 arrest associated with induction of p16ink4a and activation of RB. Oncogene. 2002; 21:5193–5203. [PubMed: 12149641]
19. Chbani L, Guillou L, Terrier P, Decouvelaere AV, Gregoire F, et al. Epithelioid sarcoma: a clinicopathologic and immunohistochemical analysis of 106 cases from the French sarcoma group. Am J Clin Pathol. 2009; 131:222–227. [PubMed: 19141382]
20. Quezado MM, Middleton LP, Bryant B, Lane K, Weiss SW, et al. Allelic loss on chromosome 22q in epithelioid sarcomas. Hum Pathol. 1998; 29:604–608. [PubMed: 9635681]
21. Zhang F, Tan L, Wainwright LM, Bartolomei MS, Biegel JA. No evidence for hypermethylation of the hSNF5/INI1 promoter in pediatric rhabdoid tumors. Genes Chromosomes Cancer. 2002; 34:398–405. [PubMed: 12112529]
22. Calderaro J, Moroch J, Pierron G, Pedeutour F, Grison C, et al. SMARCB1/INI1 inactivation in renal medullary carcinoma. Histopathology. 2012; 61:428–435. [PubMed: 22686875]
23. Rizzo D, Freneaux P, Brisse H, Louvrier C, Lequin D, et al. SMARCB1 Deficiency in Tumors From the Peripheral Nervous System: A Link Between Schwannomas and Rhabdoid Tumors? Am J Surg Pathol. 2012; 36:964–972. [PubMed: 22614000]

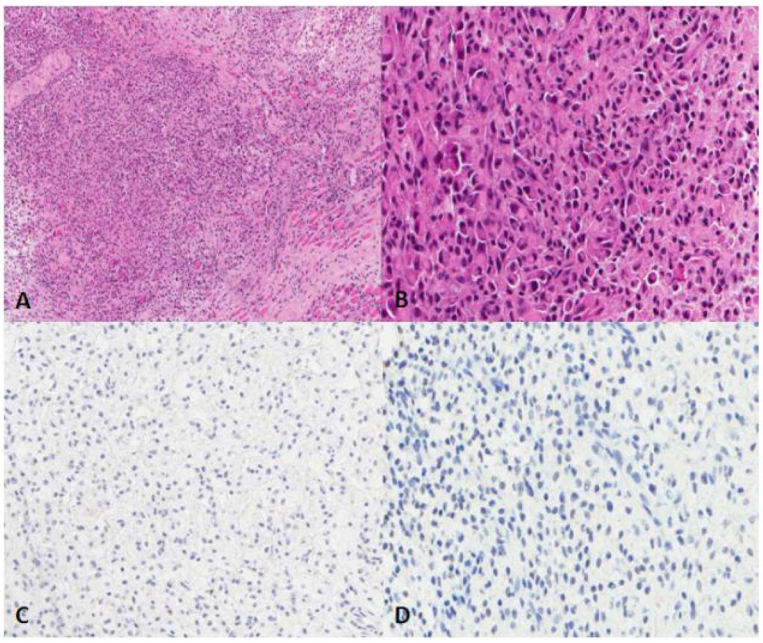

Figure 1.

The tumor consists of poorly differentiated, discohesive, medium-sized polygonal and short spindled cells with nuclear irregularity and atypia. Some of the tumor cells feature eccentric nuclei and abundant eosinophilic cytoplasm. SMARCB1 and Myogenin are negative. A. Hematoxylin and eosin (H&E) stain, 10X; B. H&E stain, 40X; C. Myogenin, 20X; D. SMARCB1, 20X.

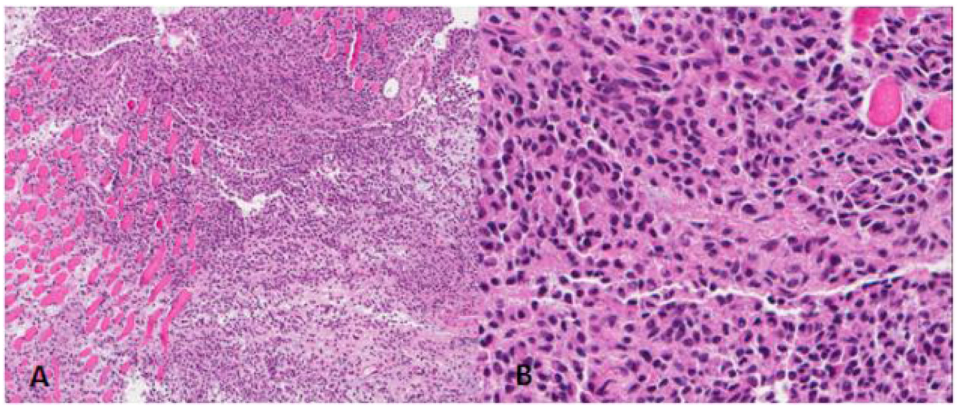

Figure 2.

The primary tumor consists of sheets of round medium to large-sized and monotonous polygonal cells with abundant weakly eosinophilic and eccentric cytoplasm and small prominent nucleoli. Focal rhabdoid features are noted. The tumor cells grow in sheets and show no glandular, papillary or squamous differentiation. A. Hematoxylin and eosin (H&E) stain, 10X; B. H&E stain, 40X.

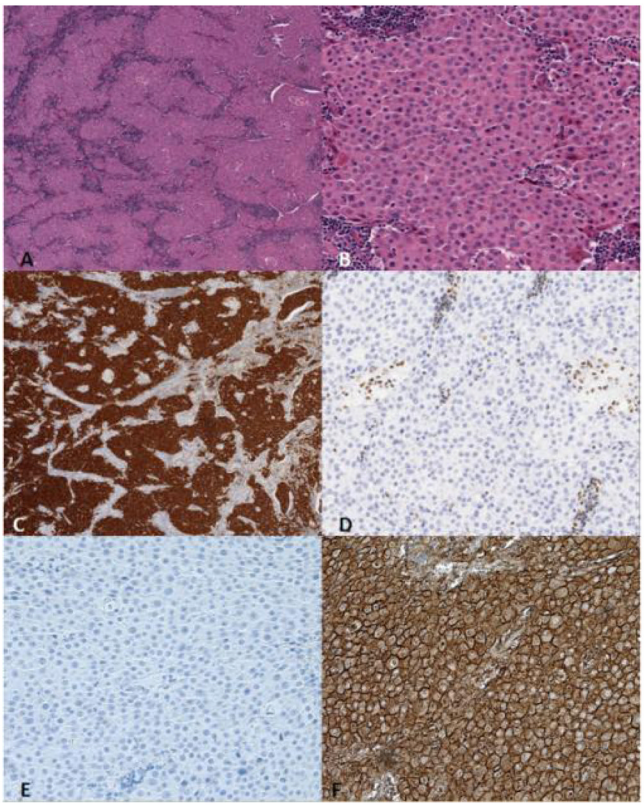

Figure 3.
The tumor consists of sheets of round medium to large-sized, monotonous polygonal cells with abundant eosinophilic cytoplasm and eccentric nuclei with small prominent nucleoli. Mitoses are rare and little necrosis is noted. Immunohistochemical (IHC) staining shows that the neoplastic cells are positive for PANCK, EMA. A. Hematoxylin and eosin (H&E) stain, 4X; B. H&E, 20X; C. PanCK 4X; D. SMARCB1, 20X; E. Desmin, 20X; F. EMA, 20X.

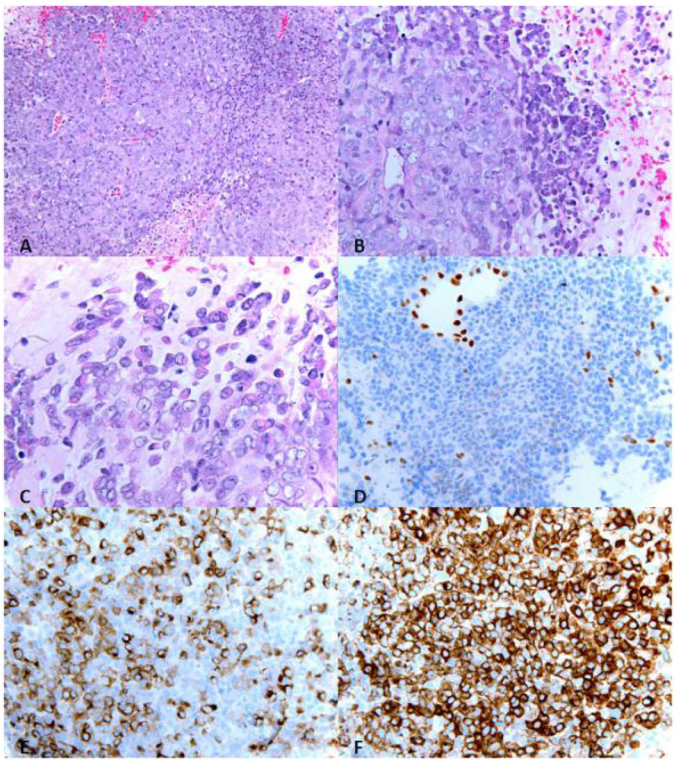

Figure 4.
The neoplasm is composed of high grade undifferentiated cells with varying amounts of eosinophilic cytoplasm, vesicular chromatin, and prominent nucleoli. Many apoptotic bodies and foci or intratumoral necrosis are seen. A minority population of cells exhibit a rhabdoid appearance with eccentric nuclei with abundant cytoplasm . A. Hematoxylin and eosin (H&E) stain, 20X; B. H&E, 40X; C. H&E, 63X; D. INI1, 40X; E. AE1/3, 40X, F. EMA, 40X.

Table 1

Immunohistochemical antibodies utilized in tumor diagnosis and classification.

IHC Marker	Dilution	Company	Antibody
AE1-3	1:400	Novocastra - NCL-AE1-AE3	AE1/AE3
BRST2	1:10	Signet 3611-1000	D6
BRST3	1:10	Signet 3612-1000	B72.3
Calretinin	1:75	Zymed-Invitrogen - 18-0211	PAD:DC8
Cam5.2	1:10	BD Biosciences - 349205	CAM5.2
CDX2	1:10	Biogenex - AM-392-5M	CDX2-88
CD1a	1:15	Novocastra - NCL-CD1a-235	MTB1
CD31	1:25	Dako - M0823	JC70A
CD34	1:80	BD Biosciences – 347660	MY10
CD68	1:2000	Dako - M0814	KP1
CEA	1:1100	Dako - A115	Polyclonal
CD163	1:50	Novocastra - NCL-163	10D6
Chromogranin	1:100	Zymed-Invitrogen - 18-0094	Polyclonal
CK5/6	1:10	Dako - M7237	D5/16/B4
CK20	1:30	Dako - M7019	K20.8
D2-40	1:25	Signet 3730-1000	D240
Desmin	1:100	Dako - M0760	D33
EBER PROBE	Ready to use	LEICA ISH5687A	N/A
Ecadherin	1:10	Dako - M3612	NCH38
EMA	1:100	Dako - M0613	E29
GFAP	1:40	Dr. John Q. Trojanowski Laboratory at HUP	2.2B10
HMB45	1:40	Neomarkers - MS-364-S	HMB45
Ini-1	1:250	BD Transduction, 612111	BAF47
Inhibin	1:30	Dako - M3609	R1
LCA	1:200	Dako - M0701	2B11&PD7/26
MelanA	1:50	Dako - M7196	A103
Myogenin	1:200	Dako, M3559	F5D
NSE	1:100	Leica NCL-NSE2	5E2
OCT-4	1:700	Santa Cruz, SC-8629	Polyclonal
P63	1:100	Biocare, CM163A	BC4A4
Panck	1:75	Biogenex, Catalog#MU357-UC	2H1
PLAP	1:50	Dako, M7191	8A9
S100	1:3750	Dako, Z0311	Polyclonal
SMA	1:600	Dako, M0851	1A4
Synaptophysin	1:50	Zymed-Invitrogen - 18-0130	Polyclonal
TLE	1:60	Santa Cruz, Sc-9121	M-101
TTF-1	Ready to Use	Dako - M3575	8G7G3/1

IHC Marker	Dilution	Company	Antibody
WT1	1:100	Dako - M3561	6F-H2

Abbreviations: IHC- immunohistochemical, HUP- Hospital of the University of Pennsylvania

Table 2

Immunohistochemical antibodies utilized in tumor diagnosis and classification for each case with results Abbreviations: IHC-immunohistochemical stain.

	Positive IHC	Focal, Weak, Equivocal IHC	Negative IHC	
Case 1	Desmin CD163 D2-40	S100 CD68 CD4	INI-1 CD35 CD21 CD31 CD138 EMA SMA Myogenin PanCK AE1/3 TTF-1 CD163 Oct4 Inhibin	CD79A CD68 CD1a LCA PAX5 Kappa Lambda IgM IgG IgA MUM1 GFAP Synaptophysin Calretinin
Case 2	PanCK CK20 CEA EMA	NSE Desmin	INI-1 S100 Mucicarmine PLAP OCT4 p63 CK7 CK5/6	CDX2 TTF-1 EBER Melan-A HMB45 Chromogranin Synaptophysin CD31
Case 3	EMA TLE-1	SMA AE1/3	INI-1 MIC2 Myogenin Desmin	TDT CD34 WT-1 Tyrosine hydroxylase